KTH ROYAL INSTITUTE
OF TECHNOLOGY

Degree project in Biotechnology

Second cycle, 30 credits

Optimization of immunotherapeutic relevant ABD-derived affinity proteins for prolonged serum half-life

EBBA BERGSTRÖM

Stockholm, Sweden 2022

Abstract

The market for protein-based drugs, or the so-called biopharmaceuticals, is a multi-billion-dollar industry today. In the development of protein-based drugs it is common to use monoclonal antibodies (mAbs) due to their ability to bind to its target with high specificity. However, therapeutical development of mAbs is limited by its long and expensive production in mammalian expression system. An alternative to mAbs are the so-called alternative scaffolds which are small proteins that can be produced in bacteria at lower costs. Although a drawback with the latter proteins is their short serum half-life. A small scaffold protein, ABD-Derived Affinity ProTein (ADAPT) of approximate 7 kDa was earlier engineered to obtain bispecific affinity, to Human Serum Albumin (HSA), to extend its half-life, as well as to the pro-inflammatory cytokine, Interleukin 17c (IL17c). Unfortunately, it was shown that the simultaneous binding was not efficient enough for its desired purpose. The aim with this project was therefore to investigate if the previous mentioned binder could be optimized by multimerization and/or manipulation of the HSA binding site for an efficient half-life extension. By generating ten new designs of the ADAPT variants, it was observed that the new variants had stable alpha helical structures and an improved or similar melting temperature as the original variant. The evaluation of the target binding displayed an improved affinity to the target, IL17c, for two of the dimeric versions as well as for the trimer and a comparable affinity for two of the monomers with a manipulated HSA binding site. The interaction to HSA was comparable to the original ADAPT for all binders except from the monomers with impaired HSA binding and the dimer with two impaired HSA binding sites. The evaluation of the simultaneous binding showed that it was favored by dimerization when a distance between the two molecule and their binding surfaces was added. Moreover, it could also be seen that the order of binding events had an impact on the simultaneous binding.

Key words: Half-Life extension, Human serum Albumin (HSA), Interleukin 17c (IL17c), ABD-Derived Affinity ProTeins (ADAPT), Protein-based drugs

Sammanfattning

Marknaden för proteinbaserade läkemedel, de så kallade biologiska läkemedlen, är idag en industri som omsätter miljarder. Ett vanligt sätt att utveckla dessa läkemedel på är med hjälp av monoklonala antikroppar då de kan binda till sitt mål med hög specificitet. Däremot begränsas denna teknik av en lång och dyr produktion som dessutom kräver däggdjursbaserade uttrycksystem. En alternativ teknik till de monoklonala antikropparna är att använda små proteiner som enkelt kan produceras i bakterier till en låg kostnad. Dock begränsas denna metod av de små proteinernas korta cirkuleringstid i blodet. I ett tidigare projekt, har ett litet protein vid namnet ABD-derived affinity ProTein (ADAPT) på cirka 7 kDa, utvecklats för att kunna binda till både humant serumalbumin (HSA) för att förlänga cirkulationstiden i blodet och Interleukin 17c (IL17c) som är ett pro-inflammatorisk cytokin. Studien visade dock att ADAPT proteinet inte samtidigt kunde binda till de båda molekylerna tillräckligt effektivt. Syftet med denna uppsats är därför att undersöka om det nämnda proteinet kan optimeras genom så kallad multimering och/eller manipulering av bindningssätet för HSA i syfte att åstadkomma en effektiv och mer långvarig cirkulationstid i blodet samtidigt som det binder sig till sitt mål, IL17c. Tio nya versioner av ADAPT proteinet har utvecklats genom att klona och transformera proteiner till en högt producerande *Escherichia coli (E. coli)* stam. Proteinerna har sedan producerats och renats fram. Det kunde observeras att proteinerna hade den önskade renheten för att kunna karaktäriseras. Vidare var det möjligt att se att proteinerna hade sin önskade molekylvikt och erhöll sin förväntade struktur som en alfahelix. Proteinernas smältpunkter hade förbättrats eller var liknande jämfört med det ursprungliga proteinet. Dessutom kunde alla proteiner återgå till sin ursprungliga struktur efter upphettning. Utvärderingen av proteinernas bindningskapacitet, med original proteinet som referens, visade på en ökad affinitet till sitt mål, IL17c, för två dimerer och trimeren samt en jämförbar affinitet för två av monomererna med ett manipulerat bindingssäte till HSA. Interaktion till HSA var jämförbar med den ursprungliga ADAPT molekylen för alla nya varianter förutom monomererna med ett manipulerat bindingssäte och dimeren med två manipulerat bindingssäten till HSA. Evaluering av de nya proteinernas kapacitet att binda samtidigt till HSA och IL17c visade att det var gynnsamt med en dimereiserad molekyl då det skapade en distans mellan molekylerna och dess bindningssäten. Vidare kunde det också visas att ordningen som molekylerna interagerade med varandra påverkade proteinernas simultana bindning.

Table of Contents

1. Introduction

The market for protein-based drugs, so called biopharmaceuticals, has grown to become a multibillion-dollar industry to this day (Precedence research, 2021). Biopharmaceuticals are drugs based on biological components, usually produced by living cells that target and interact with specific molecules in the human body with high efficiency and precision, limiting the occurrence of side-effects, to only mention one of its advantages (Kesik-Brodacka, 2018). A well renowned and top-selling biological drug is Humira® (adalimumab), a monoclonal antibody (mAb) which is currently used for the treatment of arthritic, skin, and gastrointestinal diseases (Coghlan et al., 2021). Antibodies, also known as immunoglobulins, are Y-shaped proteins produced as a response by the immune system, being able to recognize, bind, and neutralize foreign antigens. Further functions of an antibodies are their ability to recruit effector cells of the immune system as well as functioning as an adaptor protein making them multifunctional and therefore interesting in a variety of therapeutic applications (Tiller & Tessier, 2015). MAbs have a size of approximate 150 kDa and a long serum circulation, however its relatively large size reduced its ability to penetrate tissue. Additional properties of a mAb are its stable structure and low cytotoxicity and immunogenicity (Ovacik & Lin, 2018). The therapeutical development of a mAb is however limited by its expensive and long production time in mammalian expression systems (von Witting et al., 2021).

To circumvent the limitations of mAbs, another type of affinity molecules, so-called alternative scaffold proteins, can be used in the development of biological drugs. These molecules are characterized by their small size and stability enabling tissue penetration as well as the possibility to be produced in bacteria at lower cost (von Witting et al., 2021). Additionally, alternative scaffolds can be engineered to target one or multiple targets with high affinity as well, an essential feature for the development of protein-based drugs. The promising properties of the alternative scaffolds has led to the development a wide range of different non-immunoglobulin-based scaffolds, like Anticalins, Affibody molecules and DARPins to just name a few (Jost & Plückthun, 2014). The small size, however, reduces the molecules serum half-life and can lead to renal filtration (von Witting et al., 2021).

1.1 ABD- Derived Affinity ProTeins (ADAPTs) and the role of Human Serum Albumin (HSA)

One especially interesting alternative scaffold protein is the so-called ABD-Derived Affinity ProTein or ADAPT (Figure 1). This protein scaffold, with a size of approximately 7 kDa, is derived from a streptococcal protein G albumin binding domain (ABD), which can be found on the surface of gram-positive Streptococcal bacteria. The ADAPT scaffold consists out of 46 amino acids forming a left-handed three-helical structure and can, as indicated by its name, bind to Human Serum Albumin (HSA) (Linhult, et al., 2002) the most abundant protein in the human serum (Rabbani & Ahn, 2019). By

introducing another binding site opposing the binding surface to HSA, it was possible to generate a small, engineered scaffold protein, that could bind an indented therapeutic relevant target molecule as well as retain its affinity to HSA (von Witting et al., 2021).

HSA is a multifunctional, multi-domain protein of approximate 66.5 kDa (Figure 1) that can interact with a wide range of ligands and functions as a carrier for endogenous and exogenous molecules, to only mention a few of its properties. Another of HSA advantages is its long serum circulation obtained by its molecular size limiting renal clearance (Rabbani & Ahn, 2019) as well as its ability to interact with and being recycled by the neonatal Fc receptor (FcRn) and thus avoid lysosome degradation (von Witting et al., 2021). Molecular interaction to HSA is a commonly used approach for protein half-life extension, which then increases the scaffolds therapeutical relevance due to decreased renal filtration and possibly fewer administrations (Zorzi et al., 2019).

1.2 The target Interleukin 17c (IL17c)

Previously, a new ADAPT binding protein was generated to target Interleukin 17c (IL17c) a pro-inflammatory cytokine upregulated in early stages of immunological diseases such as psoriasis. IL17c (Figure 1) is a soluble homodimer expressed by mainly epithelial cells such as keratinocytes and colonic epithelial cells amongst others (Nies & Panzer, 2020).

The IL17c cytokine can signal through the receptor complex IL17RA/RE found on both epithelial cells as well as T-helper 17 (T_{h17}) cells, leading to the activation of different signaling pathways involved in the immune response. By activating the epithelial cells, the expression of IL17c is increased causing enhanced signaling which initiates cell proliferation and host defense. This is an autocrine reaction that supports the innate immune response. Furthermore, the T_{h17} activation enhances the expression of another cytokine, Interleukin 17a (IL17a), that then activates the production of other chemokines, causing a strong immune response by the adaptive immune system as well. This can also result in an hyperactivation of the immune response which in turn can lead to the development of autoimmune diseases (Nies & Panzer, 2020). The cytokine IL17c and its associated signaling axis is therefore an interesting therapeutical target.

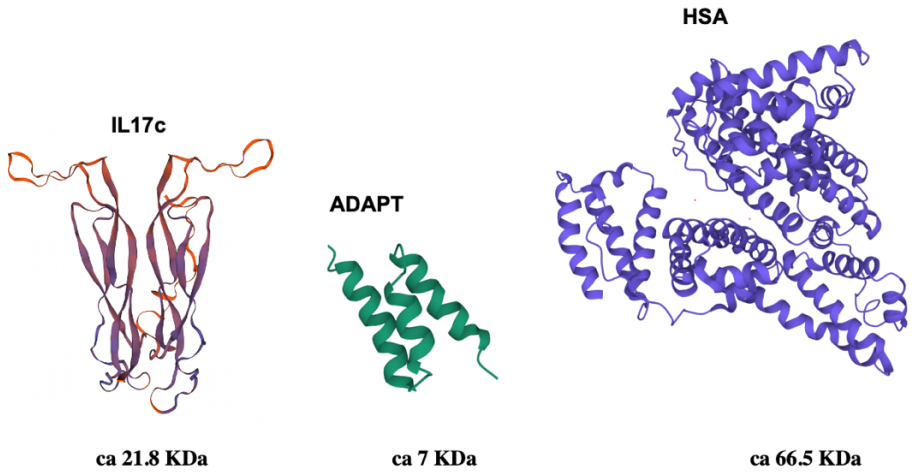

Figure 1. Schematic representation of the ABD-Derived Affinity ProTein (PDB: 1GJS) and its targets Interleukin 17c (Swiss-model: Q9P0M4) and Human serum Albumin (PDB: 1AO6). The molecular weight is shown below the molecules.

1.3 Project strategy

The aim of this project was to investigate if a previously developed ADAPT$_{_IL17c}$ binder could be optimized in order to achieve a better therapeutic potency by binding its target IL17c as well as binding to HSA for a more efficient half-life extension, making this molecule simultaneous bispecific. This was done by generating and characterizing ten new variants based on the original ADAPT$_{_IL17c}$ binder through multimerization and/or manipulation of HSA binding (Figure 2).

The first variant, the original ADAPT$_{_IL17c,}$ was used as a reference throughout this project (Wisniewski, old data). Variants 2-7 were designed as dimers of different combinations connected by a SSSG-SSSG-SSSG linker to investigate how putting a distance between two molecules and their binding surfaces could impact simultaneous binding. Further, it was also of interest to investigate if the simultaneous binding was influence by the proximity of the HSA binding site and the target binding site. Variants 4 and 6 had therefore an impaired HSA binding in the N-terminus and variant 7 in the C-terminus. Moreover, variant 5 was designed to work as a negative control with impaired HSA binding in both the N-and C-terminus whereby the impairing of the HSA binding site was based on earlier studies (Linhult et al., 2002). Variants 2 and 4 each formed a dimer together with, a previously engineered Albumin-Binding Domain with exclusive affinity to HSA, called ABD035 (Jonsson et al., 2008). Variant 8 was designed as a trimer and consists out of two ADAPTs with deleted HSA binding and one ABD035 in the middle. The remaining variants 9-11 were designed based on the already mentioned study (Linhult et al., 2002) proving that the affinity to HSA could be decreased by changing certain residues in the HSA binding site through point

mutations, which was here used to further examine how a decreased affinity to HSA could affect the ADAPTs simultaneous bispecificity.

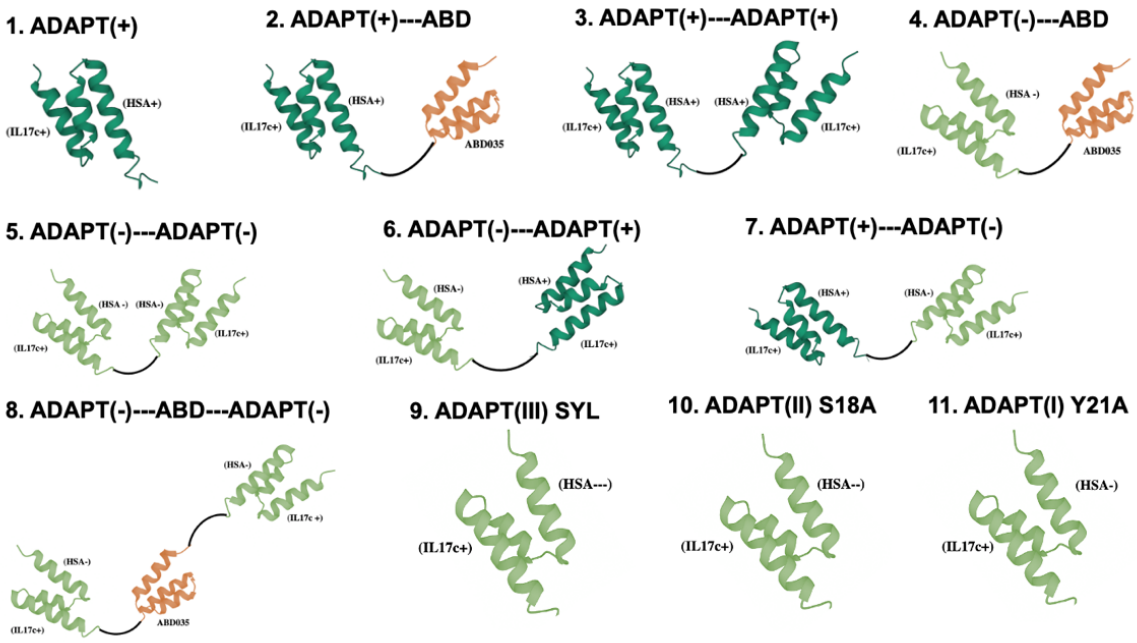

Figure 2. Schematic representation of the original variant and the 10 new ADAPT variants investigated in this project. Dark green molecule illustrates the original ADPAT_$_{IL17c}$, light green ADAPT with impaired HSA binding and the orange molecule illustrates an ABD035. The SSSG-SSSG-SSSG linker is shown in black.

The ten new variants were amplified and cloned into a DNA vector following sequence verification. To enable the production of the ADAPT variants, each gene was further cloned into a protein expression vector and thereafter the new ADAPT proteins were produced in *Escherichia coli* (*E. coli*). The purification was performed by two types of affinity chromatography and was confirmed by SDS-PAGE and Mass Spectrometry. The structural properties of the ADAPT variants were characterized by Circular Dichroism (CD) and analytical Size Exclusion Chromatography (SEC). Target binding and the evaluation of simultaneous bispecificity for each variant were determined by Surface Plasmon Resonance (SPR) and Biolayer Interferometry (BLI) respectively.

2. Materials and methods

All genes used in this project were purchased from Twist Bioscience (South San Francisco, US) and were designed to include a His-6 tag and the enzyme restriction site NcoI-HF in the N-terminus as well as enzyme restriction site XhoI in the C-terminus. The pET-45b (+) plasmid was used as vector and included carbenicillin resistance, a T7 promotor as well as matching enzyme restriction sites NcoI-HF and XhoI.

2.1 Cloning & Transformation

10 different genes were cloned into the expression vector pET-45b (+). The 10 gene inserts were first PCR amplified using Q5 DNA polymerase and thereafter analyzed for their correct size by gel electrophoresis at 180 V for 30 min. Following, QIquick PCR purification (QIAGEN) was conducted to remove old buffers and previously used enzymes. A bacterial glycerol stock containing the vector was used for plasmid amplification through inoculation in Tryptic Soy Broth (TSB) and carbenicillin (100 μg/ml) at 37 °C, 150 rpm overnight (O/N). Previously used buffers and enzymes were again removed using the QIAprep miniprep protocol (QIAGEN). Both the inserts and the vector were cleaved by double digestion using the restriction enzymes XhoI and NcoI + HF. The 10 cleaved inserts and the cleaved vector was purified by QIquick PCR purification (QIAGEN), and the vector was thereafter extracted using the QIAquick Gel extraction kit protocol (QIAGEN) from a 2% GTG agarose gel. After that, the vector (35 ng/μl) and inserts (12 ng/μl) were ligated using T4 DNA ligase. The ligation products were transformed into *E. coli* TOP10 by mixing TOP10 cells and the ligated plasmids (15-30 ng) followed by 20 min incubation on wet ice. Thereafter, the samples were heat shocked for 1 min at 42 °C and incubated for 5 min on wet ice. 250 ul of TSB was added to the samples and incubated for 1 h in a rotamixer at 37 °C, 150 rpm. The samples were plated on pre-heated agar plates containing carbenicillin and then incubated overnight at 37 °C. Single colonies were selected and screened via Colony PCR using DreamTaq DNA polymerase. Gel electrophoresis was used to confirm the insert size of each colony and the positive clones were sent for Sanger sequencing (Eurofins Genomics) to verify the correctness of the DNA sequence. The colonies with confirmed DNA sequence were then used to inoculate TSB medium containing carbenicillin (100 μg/ml) at 37 °C, 150 rpm O/N which was followed by the purification of each plasmid as described before. Thereafter, the extracted plasmids were transformed into the *E. coli* strain BL21(DE3) by using the same protocol as for the transformation into the *E. coli* strain TOP10. Colonies were selected and screened by PCR using DreamTaq DNA polymerase and the plasmid size was confirmed by gel electrophoresis again.

2.2 Protein production

First, an overnight culture was prepared for every variant by inoculating 25 ml TSB and carbenicillin (100 μg/ml) with a positive colony, that was then incubated at 37 °C, 150 rpm O/N. The following day, 250 ml cultivations each were prepared containing TSB (30g/L Tryptic Soy Broth, 5 g/L Yeast granulate), carbenicillin (100 μg/ml) and inoculated by the previously prepared overnight cultures. The cultures were grown at 37 °C until its OD_{600} had reached a value between 0.5-1.0. Isopropyl β-d-1-thiogalactopyranoside (IPTG) was added to induce the cultures followed by incubation at 25 °C, 150 rpm O/N. The proteins were harvested by centrifugation at 4000 rpm for 10 min and the obtained pellets were resuspended in either 20 ml Talon lysis buffer (7 M Guanidiniumchloride, 20 mM β-mercaptoetanol, 47 mM Na_2HPO_4, 2.65 mM $NaH2PO_4$, 10 mM Tris-HCl pH 8.0, 100 mM NaCl) or Tris-buffered saline (25 mM Tris–HCl, 200 mM NaCl, 1 mM EDTA, 0.05% (v/v) Tween20, pH 8.0) depending on the following purification method. The samples resuspended in the Talon lysis buffer were lysed by an incubation at 37 °C for 2h and the samples resuspended in TST were lysed by sonication (Vibra-cell, Sonics) with 1.0 s on/off pulse for 6 min and 39 % amplitude. Each sample was sonicated twice. Both lysis steps were followed by a centrifugation at 10000 g for 25 min and the supernatants were saved.

2.3 Protein purification

2.3.1 Human Serum Albumin (HSA) Sepharose, Tabletop purification

The produced protein variants number 2, 3, 4, 6, 7 and 8 were purified by HSA Sepharose purification using a PD10 column packed with 4 ml HSA Sepharose matrix. The HSA columns were equilibrated with 20 ml MilliQ, followed by 24 ml TST. The protein lysates were filtered using a 0.45 μm filter by a syringe and thereafter added to the columns. The columns were then washed by adding 40 ml TST each first and then 8 ml Sodium Acetate (5 mM NaOAc, pH 6.0) for desalting of the samples. Proteins bound to the column were eluted by the use of Acetic acid (0.5 M HAc, pH 2.8) in 10 fractions of 1ml each. The columns were re-equilibrated by loading 10 ml HAc, 30 ml MilliQ, 20 ml TST and 10 ml 20 % EtOH in TST onto the columns. The protein concentration for each fraction was determined by spectrophotometery (280 nm) whereby the fractions with the highest concentration were pooled together and subsequently freeze-dried (ScanVac CoolSafe freeze dryer, LaboGene). The freeze-dried samples were resuspended in Phosphate- Buffered Saline (1.5 M NaCl, 0.08 M Na_2HPO_4, 0.02 M Na_2HPO_4, pH 7.5)

2.3.2 Immobilized metal affinity chromatography (IMAC) under denaturating conditions, Tabletop purification

For protein variants number 5, 9, 10 and 11 the HSA binding site has been removed and were therefore purified using its His6-tag. PD10 columns were packed with 2 ml IMAC cobalt resin. The columns were equilibrated by adding 30 ml MilliQ and 20 ml

wash buffer (6 M Guanidiniumchloride, 50 mM Nap, 20mM Imidazole). The protein lysates were filtrated (0.45 μm) and added to the columns. 30 ml washing buffer was loaded onto the columns followed by elution of the bound proteins. The elution buffer (6 M Urea, 50 mM NaP, 300 mM NaCl, 150 mM Imidazole) was added in 10 fractions of 1 ml each. Thereafter, the columns were re-equilibrated by loading 10 ml regeneration buffer (50 mM NaP, 300 mM NaCl, 300 mM Imidazole), 30 ml MilliQ and 10 ml 20 % EtOH. The protein concentration for each fraction was determined by spectrophotometery (280 nm) and 2.5 ml of the fractions with highest concentration were pooled and buffer exchanged with PD-10 columns (Cytiva) into 3.5 ml of 5 mM Na_4Ac. The protein samples were eventually freeze dried (ScanVac CoolSafe freeze dryer, LaboGene) and resuspended in PBS.

2.4 SDS-PAGE analysis

The purified protein samples were analyzed by SDS-PAGE (Sodium Dodecyl Sulphate Polyacrylamide Gel Electrophoresis) to determine the level of purity and a first estimation of their concentration. 5 μg of each protein sample was mixed with reduction buffer (30 mM Tris-HCl, 1% SDS, 0.01% bromophenol blue, 5 mM TCEP and 13% glycerol) and boiled at 95 °C for 10 min. The samples were cooled down at room temperature and thereafter loaded onto a Mini-PROTEAN® TGX ™ (BIO-RAD) gel. The gel ran at 200 V for 30 min in 1x TGS (Bio-Rad) buffer with PageRuler Plus Prestained Protein Ladder (Thermo Scientific) as reference. The gel was washed with deionized water (3x 5 min) and stained for 1 h in GelCode Blue Safe Protein Stain (Thermo Scientific) followed by distaining in deionized water overnight.

2.5 Mass spectrometry (MS)

Electrospray ionization (ESI) MS was conducted to determine the ADAPT variants molecular weight. The systems consisted of a ProSwift RP-4H HPLC column (Thermo Scientific), an UltiMate 3000 chromatography system (Thermo Scientific), and an Impact II mass spectrometer (Bruker). All samples were diluted to a concentration of 10 pmol/ μl and processed in-house.

2.6 Circular dichroism spectroscopy (CD)

The ADAPT variant's secondary structure and melting temperature as well as their ability to refold after heat treatment was investigated by CD on a Chirascan CD spectrometer (Applied Photophysics). The protein samples were diluted to a concentration of 0.4 mg/ml in PBS. Thereafter, the secondary structure was analyzed at different wavelengths between 260 nm to 195 nm at 20 °C. Thermal stability was determined by increasing the temperature from 20 °C to 100 °C (5 °C/ min), at a constant wavelength of 221 nm. Lastly, the protein samples were cooled down to 20

°C and the refolding capacity was examined by analyze the secondary structure at different wavelengths again.

2.7 Analytical Size exclusion chromatography (SEC)

The ten proteins oligomeric state was analyzed as well as if any of the variants showed signs of aggregation. This was performed by an NGC™ Chromatography system (BIO-RAD) with a coupled Superdex 75 increase 5/150 GL column (Cytiva). 25 μl of each protein, in its current buffer (PBS) and concentration, was injected onto the system via an injection loop. A calibrant of five known protein sizes of, 75kDa, 44kDa, 13.7kDa and 6.5 kDa was used to analyze the obtained data.

2.8 Surface Plasmon Resonance (SPR)

The ADAPTs target binding to HSA and IL17c was analyzed by SPR in a Biacore 8K system (Cytiva). Variants 3-11 were diluted in Sodium Acetate (5 μg) and immobilized on a Series S sensor CM-5 chip (Cytiva). HSA and IL17c were diluted to two concentrations, 500 nM and 1000 nM, in PBS-T (1.5 M NaCl, 0.08 M Na_2HPO_4, 0.02 M Na_2HPO_4, 0.05% Tween20). The target protein was injected at a flow rate of 30 μl/ min for 120s, followed by injection of PBS-T for 240 s to monitor the dissociation. Surfaces were regenerated with 10 mM HCl in between samples.

2.9 Bio-Layer Interferometry (BLI)

Bio-Layer Interferometry was performed on an Octet^{RED}96 system (FortéBIO, PALL life sciences) to investigate the ADAPT variants simultaneous bispecificity to its targets IL17c and HSA. Two experiments were conducted to examine if the order of the binding had an impact on the simultaneous binding event as well. For both experiments the senor tips were rehydrated in StAq for at least 10 min prior to the experiment. In the first experiment, HSA (5 μg diluted in sodium acetate, pH 4.5) was immobilized on the sensor. The sensor was then incubated in PBS-T to remove excess of HSA and thereafter transferred into a solution with a variant (1000 nM) diluted in PBS-T. Afterwards, the sensor tip was moved into PBS-T to observe an occurring dissociation and then dipped in a solution of IL17c (1000 nM) diluted in PBS-T as well. Lastly the sensor tip was transferred into PBS-T for the final dissociation. The second experiment was conducted in a similar procedure, however, reversed meaning. IL17c (5 μg diluted in sodium acetate, pH 4.5) was immobilized on the sensor tip following binding to first the proteins variants (1000 nM) and secondly HSA (1000 nM).

3. Results

3.1 Cloning and transformation

Ten out of the ten new ADAPT designs were successfully cloned (Figure 3) and the DNA sequences were confirmed by Sanger sequencing. The plasmid of the original variant, which was developed prior to this project, was here used as reference. Variants 9, 10 and 11 were expected to be monomers of ca 190 bp. Variants 2, 3, 4, 5, 6 and 7 were predicted to be dimers of ca 380 bp and variant 8 a trimer of ca 560 bp.

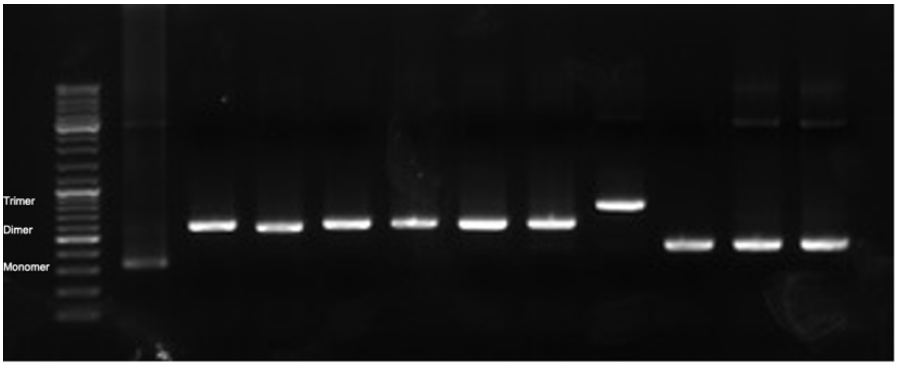

Figure 3. Result from Gel electrophoresis of the cloned plasmids. In the figure from left to right, ladder, original variant (plasmid from Wisniewski old project) followed by Plasmid 2-11. Monomer ca 190 bp, dimer ca 380 bp and trimer ca 560 bp.

3.2 Protein production and purification

In total, ten ADAPT variants were successfully produced in 250 ml cultures and purified by two different affinity chromatography techniques (HSA Sepharose and IMAC denaturation) yielding protein concentrations from 0.5 mg/ml to 12.1 mg/ml depending on the protein variant (Figure 4).

3.3 Characterization

3.3.1 Determination of the ADAPTs Molecular weight and protein purity

The molecular weight (MW) of all ADAPTs was determined by Electrospray ionization Mass Spectrometry (ESI-MS) and then compared to their calculated theoretically value (Table 1 and Table SA1). The determination of the MW was comparable, for nine out of ten variants. Variant 3 however, showed a difference of 147 Da, and could be due to that the two first amino acids in the sequenced had been proteolyzed which should not influence the target binding. This variant was therefore further analyzed.

The purity of the proteins was confirmed by SDS-PAGE and analytical SEC. The SDS-PAGE analysis showed strong bands at the expected size for ten out of ten variants (Figure 4). Furthermore, variant 2, which is a dimer, showed however strong bands at the position for both monomers and dimers which could be explained by that some of the dimers had been degraded into monomers. This variant was therefore excluded

from further characterization. Moreover, variants 9, 10 and 11, all showed a faint extra band with the same size and is most probably a cell host protein from the production in *E. coli* or a contaminant. Furthermore, the analytic SEC was conducted as a complement to examine the oligomeric state of each variant, showing if the proteins had formed aggregates, the sample was impure, or contained any host cell proteins from the production in *E. coli.* In this case, the SEC result was inconclusive.

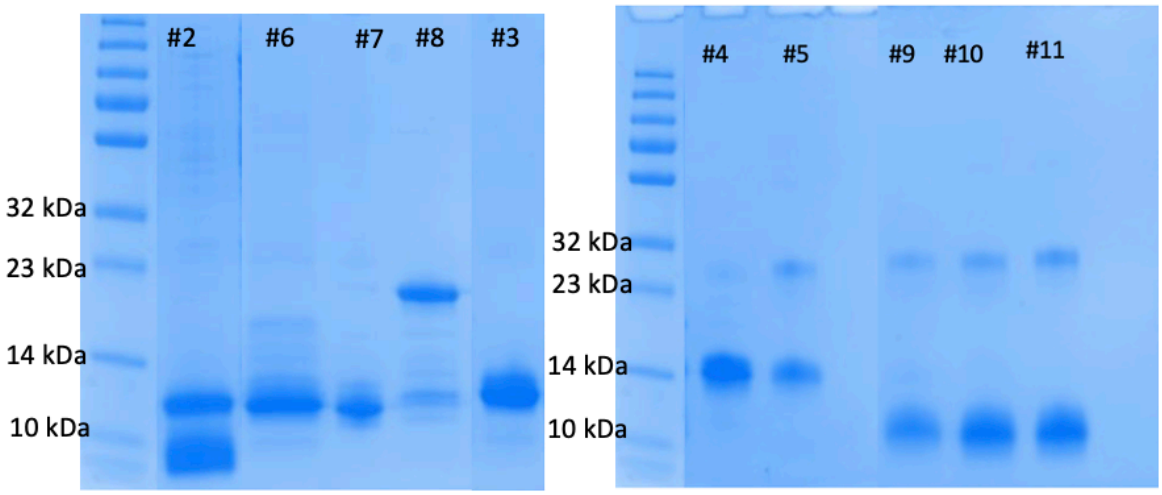

Figure 4. SDS-PAGE result showing the purity of each sample. Variants 9,10 and 11 are expected to be ca 7 kDa, variants 2, 3, 4, 5, 6 and 7 are predicted to be ca 13 kDa and variant 8 ca 19 kDa.

3.3.2 Analysis of the ADAPT variant's secondary structure and thermal stability

The CD spectroscopy experiment investigated the ADAPTs secondary structure. It was known from Wisniewski old project that the original protein, the ADAPT_$_{IL17c,}$ had an alpha helical structure and could refold following heat denaturation. Further, the experiment confirm that all nine variants displayed an alpha helical structure at 20 °C. The refolding capacity analyzed following heat denaturation, showed that the nine variants also had the ability to refold (Figure 5 and Figure SB1). However, variants 6 and 8 did not completely return to their previous state to the same extent as the other variants, although the difference was minimal. The melting temperature (Tm) differed between the different ADAPTs in a range from approximate 57 °C to 80 °C. Variant 5 had the highest melting temperature and variant 11 displayed the lowest value (Table 1). The Tm was improved for all variants compared to ADAPT_$_{IL17c}$, with a Tm of 58 °C (Wisniewski, old data), except for variants 10 and 11, where the Tm was 1 °C lower.

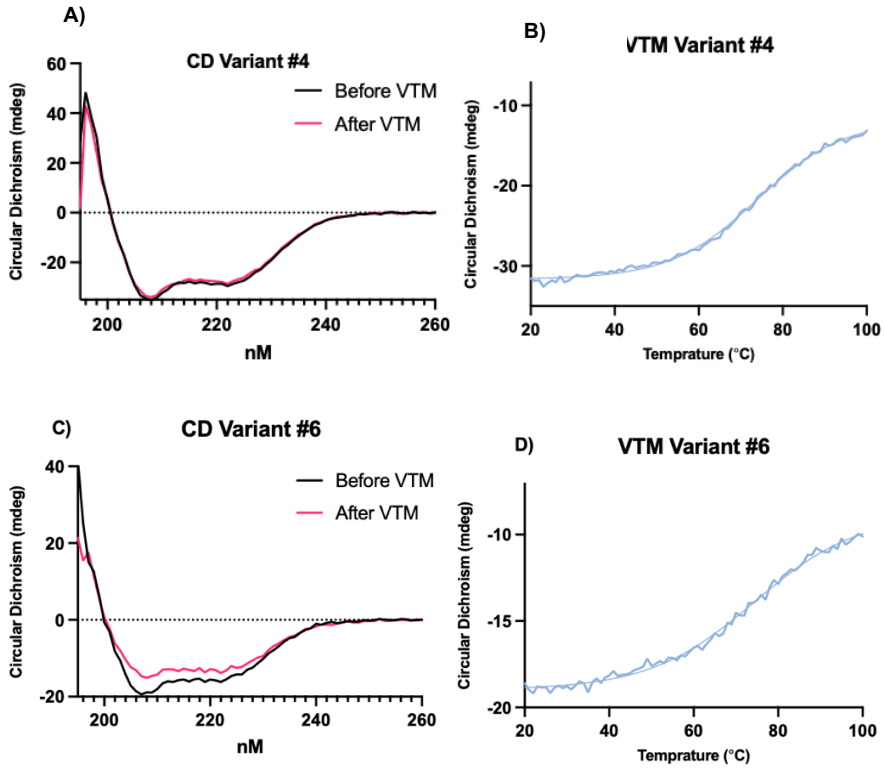

Figure 5. CD result for Variant 4 and Variant 6. (A) and (C) The secondary structure before and after Variable Temperature measurements (VTM) showing the refolding capacity. (B) and (D) VTM to determine the melting temperature of the protein. Tm for Variant 4 and Variant 6 was 73.9 ℃ and 74.4 respectively.

3.3.3 Evaluation of target binding to HSA and IL17c

The affinity measurements conducted to evaluate the target binding was performed by SPR and the dissociation equilibrium constant (KD) estimated by Biacore Insight Evaluation software. The target binding for the nine new ADAPT variants were compared to ADAPT_$_{IL17c}$ that had shown a target binding to IL17c of 1.18 x 10^{-8} M and an affinity to HSA of 3.15 x 10^{-8} M (Wisniewski, old data). Variants 3, 4, 6, 7 and 8 displayed a similar KD value in the nanomolar range for the HSA binding however, the target binding to IL17c varied. Variant 3 showed the strongest affinity to IL17c of 9.80 x 10^{-9} M and variant 11 displayed the weakest of 1.35 x 10^{-7} M (Table 1). Further, variant 4, 7 and 8 showed an improved affinity to IL17c if compared to the original variant (Wisniewski, old data). The sensorgrams (Figure 6 and Figure SC1) for the mentioned variants all had a fast on-rate and a slow off-rate for the interaction to HSA and IL17c.

Variants 5, 9, 10 and 11 were expected to have a decreased affinity to HSA which could be confirmed by the variants increased KD value compared to ADAPT_$_{IL17c}$ indicating that the affinity to HSA was decreased (Table 1). Variant 11 had the weakest affinity to HSA of 2.21 x 10^{-5} M. This could also be confirmed by the sensograms (Figure 6 and Figure SC1) displaying a fast on-rate and of off-rate implying that a very

weak interaction had occurred. The target binding to IL17c was comparable to the original variant in for variant 9, 10 and 5 and worsened for variant 11. Furthermore, the sensograms (Figure 6 and Figure SC1) showing the IL17c binding displays that an interaction has occurred with a fast on-rate and slow off-rate.

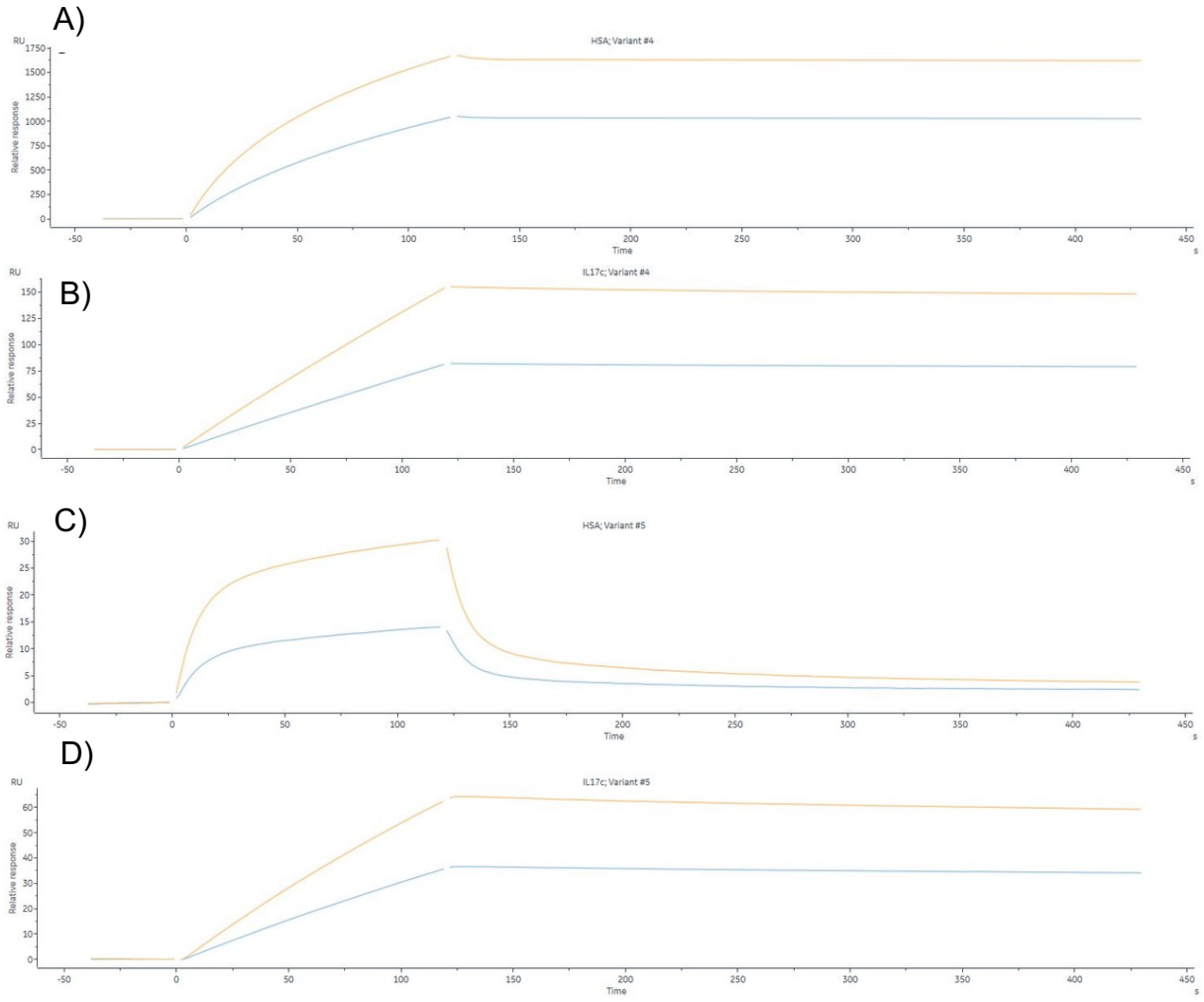

Figure 6. Senosograms from the SPR experiment showing the target binding to HSA and IL17c. Variant 4 was a dimer of two ADAPTs and variant 5 was a dimer of two ADAPT with impaired HAS binding. A) and C) Variants 4 and 5 target binding to HSA. B) and D) Interaction between IL17c and variant 4 and 5 respectively.

Table 1. A data summary of the above-mentioned results. The table shows the molecular weight (MW) determined by the ESI MS, the structure, melting temperature and refolding capacity evaluated by the CD experiment and the affinity measurements (KD-values) obtained by the SPR experiment.

Variant	Name	MW [Da]	Helical structure	Tm [°C]	Refolding capacity	KD [M] IL17c	KD [M] HSA
Variant #3	ADAPT(+) --- ADAPT(+)	13206.9	Yes	66.5	Yes	9.80×10^{-9}	1.19×10^{-8}
Variant #4	ADAPT(-) --- ABD	13060.8	Yes	73.9	Yes	6.22×10^{-8}	1.64×10^{-8}
Variant #5	ADAPT(-) --- ADAPT(-)	13108.8	Yes	79.9	Yes	3.63×10^{-8}	3.31×10^{-6}
Variant #6	ADAPT(-) --- ADAPT(+)	13157.9	Yes	74.4	Yes	3.16×10^{-8}	1.74×10^{-8}
Variant #7	ADAPT(+) --- ADAPT(-)	13157.9	Yes	72.4	Yes	9.47×10^{-9}	3.49×10^{-8}
Variant #8	ADAPT(-) --- ABD --- ADAPT(-)	19155.7	Yes	73.0	Yes	7.74×10^{-9}	3.46×10^{-8}
Variant #9	ADAPT(-) (III) SYL	7013.9	Yes	68.9	Yes	1.45×10^{-8}	8.1×10^{-6}
Variant #10	ADAPT(-) (II) S18A	7046.9	Yes	57.3	Yes	1.17×10^{-8}	3.48×10^{-7}
Variant #11	ADAPT(-) (I) Y21A	6970.8	Yes	56.7	Yes	1.34×10^{-7}	2.21×10^{-5}

3.3.4 Evaluation of simultaneous bispecificity to HSA and IL17c

The SPR data analyzed the nine ADAPT variant's ability to bind to HSA and IL17c respectively. To further evaluate simultaneous bispecificity a Biolayer Interferometry was conducted. Two experiment was performed with either HSA or IL17c on the tip to examine how the order of the binding events might affected the simultaneous bispecificity. The original variant in this project, ADAPT$_{IL17c,}$ was used as a reference and showed simultaneous binding, 0.24 nm, when HSA was immobilized on the tip however not in the reversed experiment with IL17c on the tip (Wisniewski, old data).

While HSA was on the tip, simultaneous binding could be seen for the majority of the variants. However, while IL17c was on the tip, the affinity to HSA decreased, resulting in a declined simultaneous specificity for mostly all of the tested ADAPTs. Furthermore, when comparing the new ADAPT designs to ADAPT$_{IL17c}$, two variants, number 5 and 8 showed no simultaneous binding in the two experiments. Variant 5 was designed to have no binding to HSA which could be confirmed by the fast off-rate in sensogram B (HSA on tip) and the lack of the binding event in sensogram D (IL17c on tip). Additionally, variant 5 also displayed low affinity to IL7c in both experiments. Variant 8 had affinity to both HSA and IL17c however, did not require the ability to bind both binding partners simultaneously (Figure 7). Variant 4, 9, 10 and 11 showed simultaneous bispecific while HSA was immobilized on the tip (Figure 7) although, with a response below 0.24 nm.

The simultaneous binding for variant 3, 6, and 7 was improved with immobilized HSA on the tip. In contrast, while IL17c was immobilized on the tip, variant 3 displayed strong binding to IL17c however a decreased binding to HSA. Similar result could be seen for variant 6 and 7 although with a lower response.

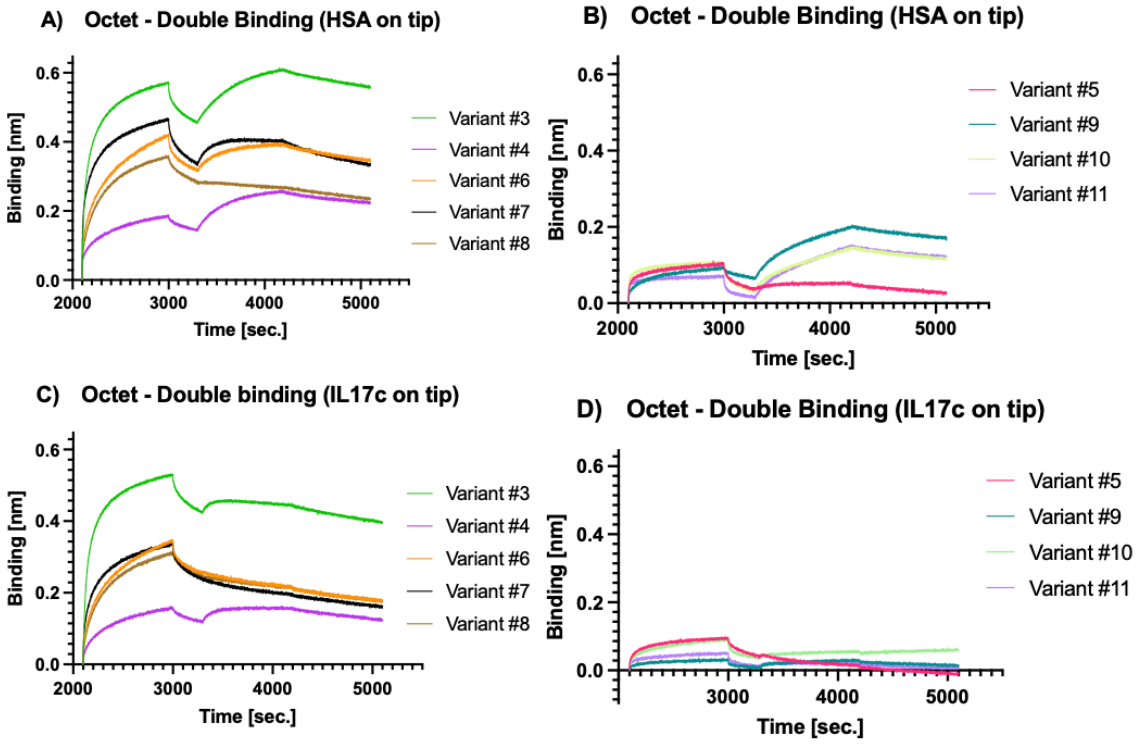

Figure 7. Evaluation of simultaneous target binding to IL17c and HSA. (A) and (B) HSA immobilized on the senor tip. First peak illustrates the binding event between HSA and the respective Variants. Peak two illustrated the binding event between the HSA-ADAPT complex and IL17c. (C) and (D) Reversed experiment. First peak, interaction between IL17c and the ADAPT. Second peak, interaction between the IL17c-ADAPT complex and HSA..

4. Discussion

The project aim was to optimize the immunotherapeutic ADAPT$_{_IL17c}$ binder by prolonging its human serum half-life. ADAPTs are small molecules (ca 7 kDa) with fast blood clearance if not engineered to interact with certain other proteins like albumin, enabling for a possible half-life extension. This well- known approach has been applied here by the use of ADAPT binding proteins. Fast blood clearance can however be beneficial for other application such as molecular imaging where the latter in combination with small proteins ability to penetrate tissue results in high resolution images. In an earlier study, the ADAPT$_{_IL17c}$ scaffold has been engineered to become bispecific, targeting both HSA and its target IL17c, however not with a desired efficiency (von Witting et al., 2021). Therefore, in this project, 10 new ADAPT designs has been generated to evaluate this half-life extension strategy for small bispecific proteins.

The production and purification steps resulted in varying protein concentrations between the variants as well as difference in purity shown by the SDS-PAGE analysis. This could have been influenced by the variants different production efficiency and the use of different purification methods. Most of the variants were purified by HSA Sepharose chromatography, a method that exploits a proteins affinity to HSA resulting in pure samples. Variant 5, 9, 10, 11 however, were purified by IMAC due to their impaired HSA binding. The IMAC purification required optimization and was performed in denaturating conditions, by adding UREA and guanidinium hydrochloride to the buffers, to reach the desired purity. Denaturating conditions can be used when a protein is expressed at high levels and aggregates in insoluble inclusion bodies and facilitates the purification by exposing the proteins His-tags (Spriestersbach et al., 2015). The purification step was analyzed by SDS-PAGE confirming that all protein variants showed bands at the expected size. Unfortunately, bands of other sizes could be detected for some of the variants as well, showing that an optimization of the protein purification for future experiments might be needed. An additional validation was performed by ESI-MS and it could be observed that the determined molecular weight was comparable to the theoretical value for nine out of ten proteins, indicating that the desired protein variants had been produced. Variant 3 had a higher calculated MW than the measured value by ESI-MS. This could be explained by proteolysis of the first two amino acid in the sequence although it should not affect the target binding.

All the generated ADAPT variants displayed an alpha helical structure and the ability to refold after heat treatment, indicating that the variants had a stable structure. The original ADAPT had a melting temperature of 58 °C which was improved for eight variants and similar for the remaining two (Table 1). The improved melting temperature could be due to the larger molecular size obtained by multimerization (Watson et al., 2018). Additionally, it can be shown that neither the dimerization, trimerization nor the impairing of the HSA binding site affected the variants stability.

Further, the binding properties for each variant was evaluated by SPR. The variants that were dimerized and trimerized by adding another ADAPT resulted in a molecule

with two binding surfaces to IL17c which could theoretically improve the target binding. Variant 3 was a dimerized version of the original construct and showed the highest affinity to the target IL17c, a KD of 9.80 x 10^{-9} M, and did however, not show any signs of an improved affinity to HSA if compared to the original variant. Variants 6 and 7 were dimerized by linking an ADAPT with impaired HSA binding in the N- or C-terminus respectively. Both variants had an improved affinity to IL17c although Variant 7 had a KD of 9.47 x 10^{-9} M, a tenfold increase compared to Variant 6. This indicated that the location of the impaired HSA binding has an impact on the IL17c binding site and that the dimerized structures are favoured, in terms of target binding, by impairing the HSA binding in the C-terminus. Moreover, the binding to HSA for both variant 6 and 7 was comparable to the original variant and was in the nanomolar range. Variants 4 were dimerized by linking a ABD035 to an ADAPT and an affinity to HSA in the nanomolar range could be observed, which was expected since ADB035 has a femtomolar affinity to HSA by itself (Jonsson et al., 2008). Furthermore, variant 4, with an impaired HSA binding in the N-terminus of the ADAPT, displayed a similar target binding to IL17c as the original variant. Variant 8 was trimerized although the complex was still smaller than a mAb. This variant consisted out of two ADAPTS with impaired HSA binding and an additional ABD035 and showed an improved target binding to IL17c of 7.74 x 10^{-9} M and a similar affinity to HSA as the original variant. Some of the multimerized structures could demonstrated an improved efficacy of the target binding, however, the binding affinity to HSA was always comparable to the original construct. This result was similar to an earlier study performed by Garousi et al., 2019, investigating the role of a dimerized ADAPT targeting Human Epidermal Growth Factor 2 (HER2), where an increased affinity to the target could be observed when the ADAPT was dimerized by an optimal linker.

Variants 5, 9,10 and 11 were, as mentioned before, designed to not have, or have a weakened affinity to HSA. The target binding to IL17c was comparable to the original binder for variants 5, 9 and 10 and worsened for variant 11 indicating that amino acid substitution could have had an impact on the proteins charge and by that also the target binding. The impairing of the HSA binding was based on an earlier study (Jonsson A et al, 2008). In our study, it could be observed that the affinity to HSA was worsened for all four constructs however, not in agreement with the earlier study. Variants 5 and 9 should have had the worse affinity to HSA although this was however, shown for variant 11 with a KD of 2.21 x 10^{-5} M. The HSA impairing in the multimers, discussed earlier, was based on the same amido acid substitution as for variant 5 and 9 and should be taken into consideration when evaluating their affinity to HSA. An additional aspect of the SPR experiment is the impact of the immobilization step. In this study, each variant was immobilized on the chip and fixated the structures in a certain position and thus limited the proteins flexibility. Due to this, the interaction could have been influenced and potentially decrease its binding capacity to each target. The reversed experiment, with immobilized HSA and IL17c, was performed in this project however, due to technical issue it could not be analysed properly.

The evaluation of the simultaneous binding was performed by BLI. This experiment could examine if additional factors as steric hindrance could affect the simultaneous binding as well as the order of the binding events. HSA is the most abundant protein in the human serum (Zorzi et al., 2019) and would most probably be the first molecule that the ADAPT binder interacted with following administration. Therefore, the BLI experiment with immobilized HSA is mimicking the human body the best and should be the experiment in focus. Moreover, the BLI experiment with immobilized IL17c should be evaluated as a complement. Here, we could demonstrate that the simultaneous binding could be improved for variants 3, 6 and 7 and thus by dimerization. Moreover, variant 3 showed a fast on-rate when binding to first HSA and secondly to IL17c following a slow off-rate which is a desirable feature for a therapeutical protein (Figure 7). In contrast, when IL17c was immobilized on the sensor tip, it could be observed that the on-rate when binding to the second target, HSA, was decreased and could be due to sterically hindrance consequently by the proteins flexibility. If comparing variant 6 and 7, three variants that also had improved simultaneous binding compared to the original variant, it can be observed that variant 7 had the highest on-rate of ca 0.5 nm, with immobilized HSA. However, neither variants 6 nor 7 had the ability to bind HSA when first interacting with IL17c. However, the SDS-PAGE gel (Figure 4) displayed that bands had appeared at both the positions for the monomer and the dimer, and the data can't thus not be trusted completely.

In a previous study by Malm et al., 2014, two affibodies were linked to an ABD035 for simultaneous bispecificity to two tumor antigens and demonstrated simultaneous binding in its trimeric state. This is however, not in agreement to the results in this project showing that 8, the trimer, did not have the ability to bind the target IL17c and HSA simultaneously and is most probably due to sterically hindrance between the domains. It could therefore be of relevance to examine different length of the linkers to find an optimal proximity of the three molecules in order to achieve simultaneous binding. Furthermore, evaluating the simultaneous binding of the variants 5, 9, 10 and 11 with impaired HSA binding, both as monomers and dimers, it could be observed that the binding was not improved if compared to the original variant and therefore seems not to be a potential strategy for an efficient half-life extension in this case.

To conclude this project, the most promising strategy for half-life extension of an immunotherapeutic ADAPT protein is dimerization by linking an ADAPT to another ADAPT and thus creating a distance between the two molecules and their binding surfaces. Furthermore, this study also revealed that if the ADAPT binds first to IL17c it will hinder the ADAPT from binding to HSA, which was not the case for the revered binding event. A distance is required for an efficient simultaneous binding and variant 3 has shown to have the most promising structure. Additionally, an improvement could also be observed for variants 6 and 7 and could be interesting to analyze in a further study.

5. Future perspectives

This project has contributed to the field of protein technology by focusing on half-life extension of small protein binders and has resulted in an overview of the role of ADAPT multimerization and manipulation of the HSA binding site. Three out of the ten generated new variants showed promising improvements that could be of interest for further analysis.

In a further project, the first step could be to optimize the purification process by either use a newly made HSA Sepharose matrix or by using the IMAC purification method under denaturating conditions. An efficient purification process is important in order to acquire valid and accurate results in the characterization process. An additional experiment analyzing the potential formation of aggregates by Size Exclusion Chromatography could be performed as a complement to the CD data determining the structural properties of the proteins.

The target binding analyzed by SPR could be improved by adding a larger variety of concentrations of HSA and IL17c as well as performing a reversed experiment immobilizing the target proteins on the chip instead of each variant. By adding more concentrations of the target, it could be possible to analyze the sensitivity of the binding as well as to get more detailed information about the exact affinity of the molecules to each other. The reversed experiment is of interest to include the aspect of protein flexibility and movement in the 3D space. Moreover, if a distinction in the affinity could be observed a further experiment of the simultaneous bispecificity could be performed by BLI to further evaluate the impact of the ratio between HSA and IL17c. The ADAPT proteins are developed for therapeutical applications, and it could therefore be of relevance to examine the sensitivity to further understand at what level IL17c must be expressed in order for a simultaneous binding to occur. A detailed evaluation of the binding would lead to the next step in the research process analyzing the effectivity and binding affinity in mammalian cells and could be performed by a mammalian cell assay.

6. Acknowledgment

First, I want to acknowledge Sophia Hober for giving me the chance to perform this project and for all the feedback I have received. Further, I want to give a big thanks to my supervisor Andy for your engagement from the start until the end, and for being an inspiring and encouraging teacher. I have learnt a lot from you these couple of weeks. I would also like to acknowledge the Hober lab group for your insights, tips and kindness throughout this project and Floor 3 for being a fun and motivating place to work. Finally, I want to thank Gabriella Jensen for your help with my MS samples.

References

Coghlan, J., He, H., & Schwendeman, A. S. (2021). Overview of Humira® Biosimilars: Current European Landscape and Future Implications. *Journal of Pharmaceutical Sciences*, *110*(4), 1572–1582. https://doi.org/10.1016/j.xphs.2021.02.003

Garousi, J., Lindbo, S., Borin, J., von Witting, E., Vorobyeva, A., Oroujeni, M., Mitran, B., Orlova, A., Buijs, J., Tolmachev, V., & Hober, S. (2019). Comparative evaluation of dimeric and monomeric forms of ADAPT scaffold protein for targeting of HER2-expressing tumours. *European Journal of Pharmaceutics and Biopharmaceutics*, *134*, 37–48. https://doi.org/10.1016/j.ejpb.2018.11.004

Jonsson, A., Dogan, J., Herne, N., Abrahmsen, L., & Nygren, P.-A. (2008). Engineering of a femtomolar affinity binding protein to human serum albumin. *Protein Engineering Design and Selection*, *21*(8), 515–527. https://doi.org/10.1093/protein/gzn028

Jost, C., & Plückthun, A. (2014). Engineered proteins with desired specificity: DARPins, other alternative scaffolds and bispecific IgGs. *Current Opinion in Structural Biology*, *27*, 102–112. https://doi.org/10.1016/j.sbi.2014.05.011

Kesik-Brodacka, M. (2018). Progress in biopharmaceutical development. *Biotechnology and Applied Biochemistry*, *65*(3), 306–322. https://doi.org/10.1002/bab.1617

Linhult, M., Binz, H. K., Uhlén, M., & Hober, S. (2002). Mutational analysis of the interaction between albumin-binding domain from streptococcal protein G and human serum albumin. *Protein Science*, *11*(2), 206–213. https://doi.org/10.1110/ps.02802

Malm, M., Bass, T., Gudmundsdotter, L., Lord, M., Frejd, F. Y., Ståhl, S., & Löfblom, J. (2014). Engineering of a bispecific affibody molecule towards HER2 and HER3 by addition of an albumin-binding domain allows for affinity purification and in vivo half-life extension. *Biotechnology Journal*, *9*(9), 1215–1222. https://doi.org/10.1002/biot.201400009

Nies, J. F., & Panzer, U. (2020). IL-17C/IL-17RE: Emergence of a Unique Axis in TH17 Biology. *Frontiers in Immunology*, *11*. https://doi.org/10.3389/fimmu.2020.00341

Ovacik, M., & Lin, K. (2018). Tutorial on Monoclonal Antibody Pharmacokinetics and Its Considerations in Early Development. *Clinical and Translational Science*, *11*(6), 540–552. https://doi.org/10.1111/cts.12567

Rabbani, G., & Ahn, S. N. (2019). Structure, enzymatic activities, glycation and therapeutic potential of human serum albumin: A natural cargo. *International Journal of Biological Macromolecules*, *123*, 979–990. https://doi.org/10.1016/j.ijbiomac.2018.11.053

Spriestersbach, A., Kubicek, J., Schäfer, F., Block, H., & Maertens, B. (2015). *Purification of His-Tagged Proteins* (pp. 1–15). https://doi.org/10.1016/bs.mie.2014.11.003

Tiller, K. E., & Tessier, P. M. (2015). Advances in Antibody Design. *Annual Review of Biomedical Engineering*, *17*(1), 191–216. https://doi.org/10.1146/annurev-bioeng-071114-040733

von Witting, E., Lindbo, S., Lundqvist, M., Möller, M., Wisniewski, A., Kanje, S., Rockberg, J., Tegel, H., Åstrand, M., Uhlén, M., & Hober, S. (2021). Small Bispecific Affinity Proteins for Simultaneous Target Binding and Albumin-Associated Half-Life Extension. *Molecular Pharmaceutics*, *18*(1), 328–337. https://doi.org/10.1021/acs.molpharmaceut.0c00975

Watson, M. D., Monroe, J., & Raleigh, D. P. (2018). Size-Dependent Relationships between Protein Stability and Thermal Unfolding Temperature Have Important Implications for Analysis of Protein Energetics and High-Throughput Assays of Protein–Ligand Interactions. *The Journal of Physical Chemistry B*, *122*(21), 5278–5285. https://doi.org/10.1021/acs.jpcb.7b05684

Zorzi, A., Linciano, S., & Angelini, A. (2019). Non-covalent albumin-binding ligands for extending the circulating half-life of small biotherapeutics. *MedChemComm*, *10*(7), 1068–1081. https://doi.org/10.1039/C9MD00018F

Precedence research (2021). Biopharmaceutical Market Size to Hit US$ 856.1 Bn by 2030. GlobalNewswire. https://www.globenewswire.com/newsrelease/2021/12/22/2357003/0/en/Biopharmaceutical-Market-Size-to-Hit-US-856-1-Bn-by-2030.html

Supplementary Figures and Tables

A. Molecular weight

Table SA1. The theoretical calculated molecular weight for each construct and the measured molecular weight by ESI MS.

Variant	Name	Theoretical MW (Da)	Measured MW (Da)
Variant #2	ADAPT(+) --- ABD	13109.8	13109.7
Variant #3	ADAPT(+) --- ADAPT (+)	13206.9	13059.8
Variant #4	ADAPT (-) --- ABD	13060.77	13059.7
Variant #5	ADAPT (-) --- ADAPT (-)	13108.82	13107.5
Variant #6	ADAPT (-) --- ADAPT (+)	13157.89	13157.5
Variant #7	ADAPT (+) --- ADAPT (-)	13157.89	13157.5
Variant #8	ADAPT (-) --- ABD --- ADAPT (-)	19155.69	19154.8
Variant #9	ADAPT (-) (III) SYL	7013.90	7013.5
Variant #10	ADAPT (-) (II) S18A	7046.97	7046.5
Variant #11	ADAPT (-) (I) Y21A	6970.82	6969.4

B. Circular Dichroism

The figures below show the results from the CD experiment.

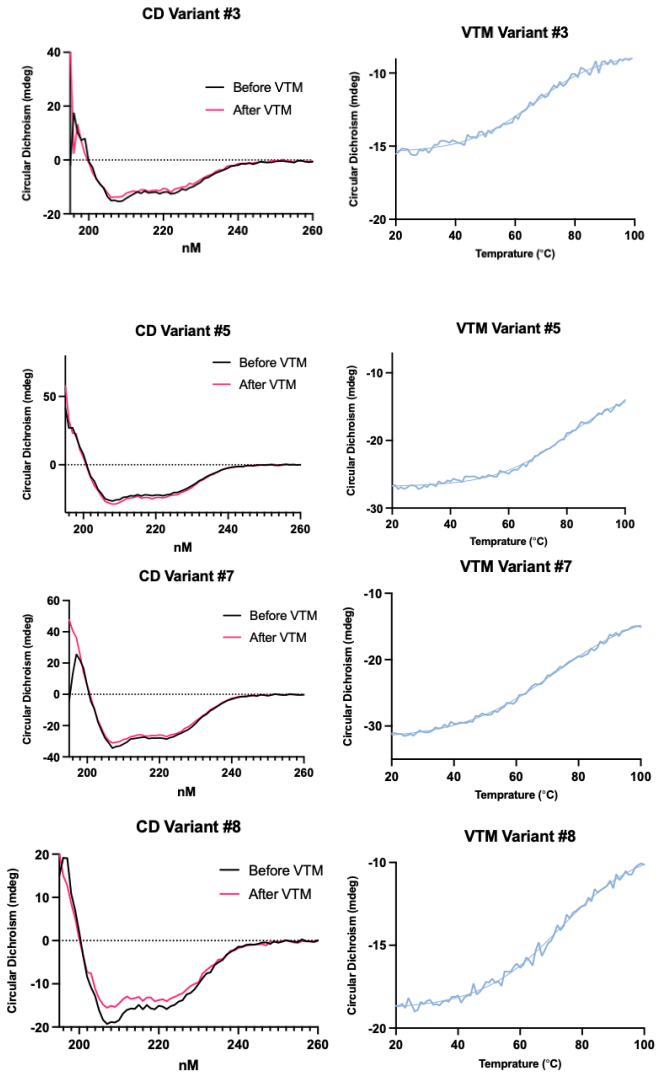

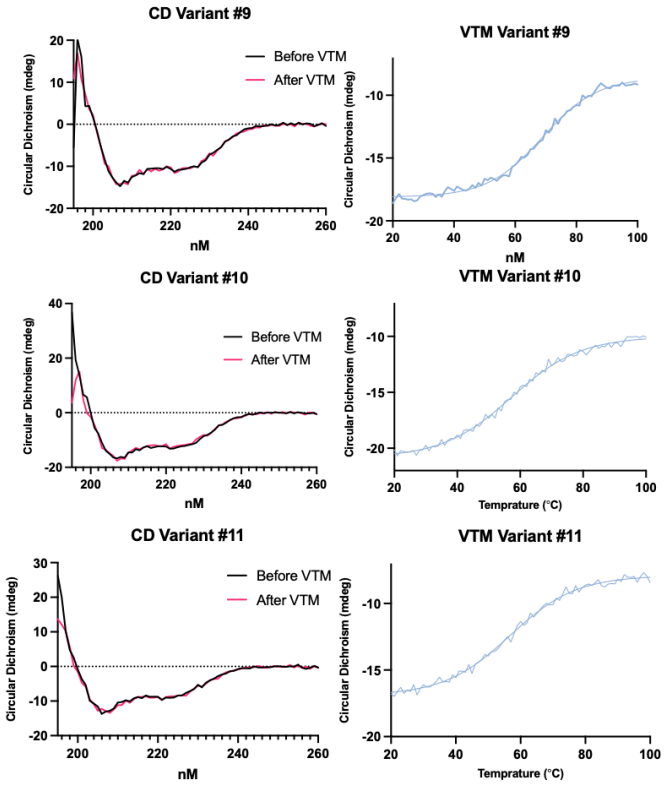

Figure SB1. Graphs displaying each variant's secondary structure, refolding capacity, and melting temperature.

C. Surface Plasmon Resonance

Below is the sensograms retrieved from the SPR experiment and shows the binding between each variant and its target bindings HSA and IL17c.

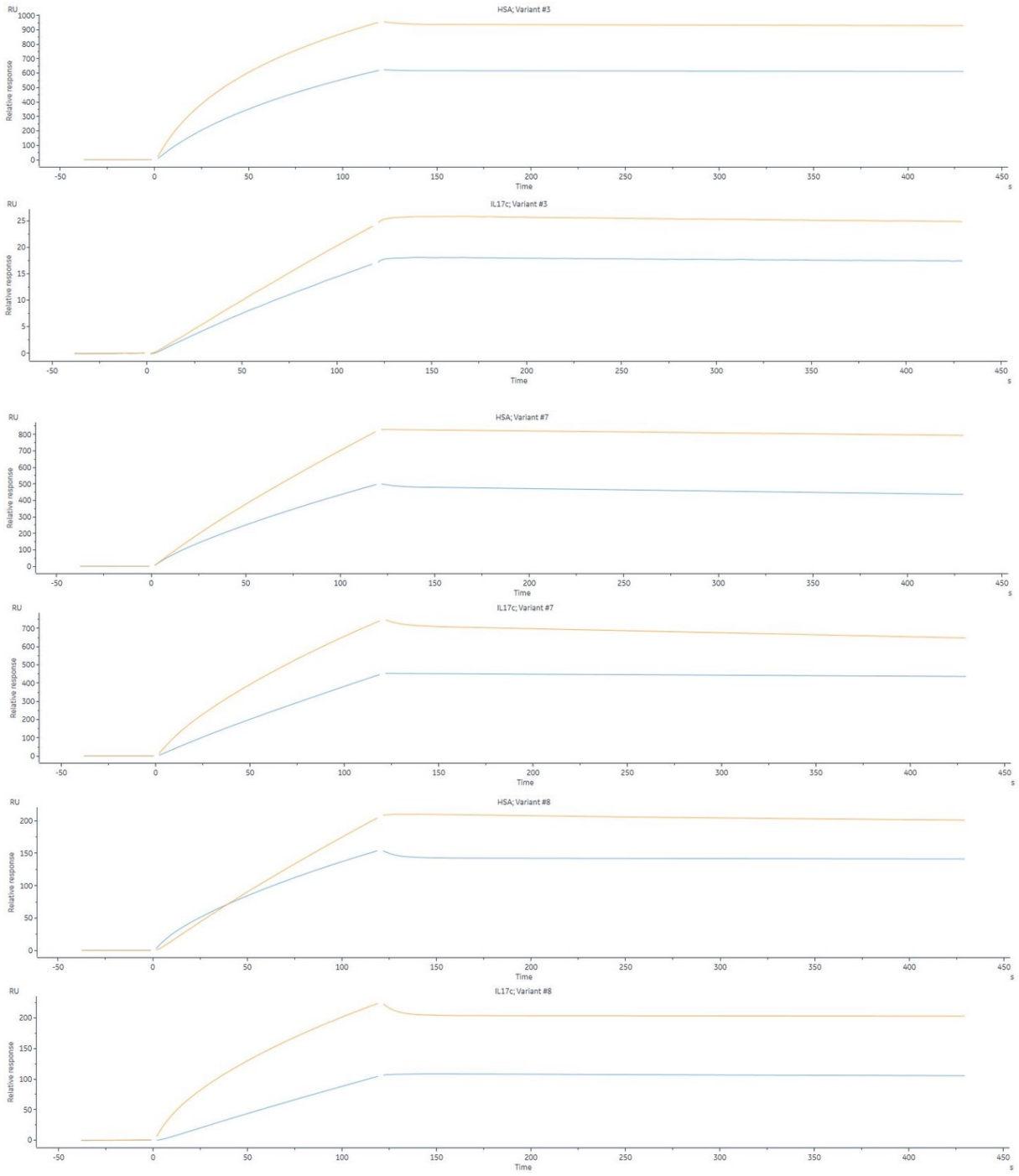

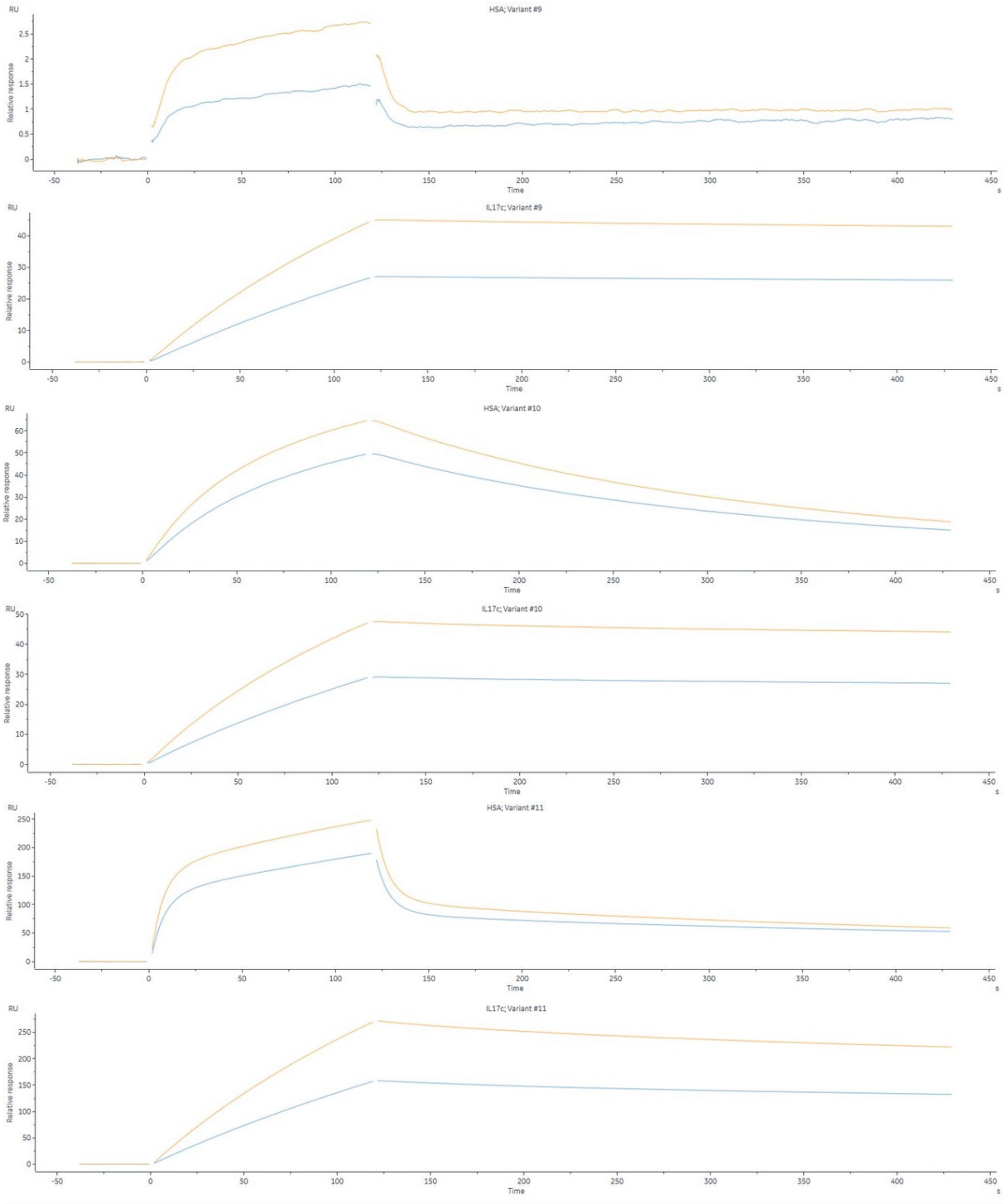

Figure SC1. Results from the SPR experiment showing each variants target binding to HSA and IL17c.